Neurobiology of Aging 161 (2026) 64–72

Contents lists available at ScienceDirect

Neurobiology of Aging

journal homepage: www.elsevier.com/locate/neuaging.org

ABCA7 rs115550680 risk allele carriers have lower medial temporal lobe dynamic network flexibility than *APOE-ε4* allele carriers among older African Americans

Miray Budak [a,*,1], Bernadette A. Fausto [a,2], Victoria Paruzel [a,3], Payton White [a,4], Martina Ishaq [a,5], Soodeh Moallemian [a,6], Kelly N. Nudelman [b,7], Mark A. Gluck [a,8]

[a] Center for Molecular and Behavioral Neuroscience, Rutgers University–Newark, 197 University Ave., Suite 209, Newark, NJ 07102, USA
[b] Department of Medical and Molecular Genetics, Indiana University School of Medicine, 410 W. 10th Street, Indianapolis, IN 46202, USA

ARTICLE INFO

Keywords:
Alzheimer's disease
ABCA7
APOE-ε4
Medial temporal lobe
Network flexibility
Dynamic functional connectivity
African Americans

ABSTRACT

Alzheimer's disease (AD) pathology disrupts functional brain connectivity long before symptoms emerge. African Americans face elevated AD risk, yet underlying mechanisms remain unclear. Genetic risk differs by ancestry: *APOE-ε4* strongly predicts late-onset AD in European ancestry, whereas *ABCA7 rs115550680* confers substantial risk in African ancestry. Yet, how these variants influence neural function in African Americans is unclear. The medial temporal lobe (MTL) is an early target of AD pathology and resting-state functional Magnetic Resonance Imaging (rs-fMRI) measures of dynamic network connectivity (hereafter "flexibility"), the brain's capacity to dynamically reconfigure connectivity, provide a sensitive metric of network adaptability, potentially preceding structural decline. However, comparative influence of *APOE-ε4* and *ABCA7 rs115550680* on MTL flexibility and subregional volumes in this population is unknown. 146 older African Americans ($Mean_{Age}$=69.71 $Mean_{SD}$=6.29) were genotyped for *APOE-ε4* and *ABCA7 rs115550680* via saliva samples. Rs-fMRI was used to calculate MTL flexibility and T1-weighted MRI quantified MTL subregional volumes. ANCOVAs controlled for age, sex, and education, and *APOE-ε4* when *ABCA7 rs115550680* was the predictor. *ABCA7 rs115550680* risk allele carriers exhibited lower MTL flexibility than non-carriers ($p = .042$) and *APOE-ε4* allele carriers ($p = .030$). They also showed hypertrophy in left anterior hippocampus ($p = .049$), bilateral entorhinal cortex (ERC) (right $p = .048$; left $p = .020$) compared to non-carriers, and greater left ERC volume than *APOE-ε4* allele carriers ($p = .027$). *APOE-ε4* or interaction effects were not significant ($p > .05$). These findings provide preliminary evidence that *ABCA7 rs115550680* risk allele, but not *APOE-ε4* allele, is linked to reduced MTL flexibility and subregional hypertrophy in older African Americans, suggesting ancestry-specific mechanisms of early AD risk.

1. Background

Older African Americans experience disproportionately high rates of Alzheimer's disease (AD) compared to other racial and ethnic groups in the United States (Barnes, 2022). The prevalence of AD is almost twice as high in this population, yet the neural and genetic mechanisms

* Corresponding author.
E-mail addresses: miray.budak@rutgers.edu (M. Budak), bernadette.fausto@rutgers.edu (B.A. Fausto), wtp18@newark.rutgers.edu (V. Paruzel), pw352@newark.rutgers.edu (P. White), martina.ishaq@rutgers.edu (M. Ishaq), s.moallemian@rutgers.edu (S. Moallemian), kholohan@iu.edu (K.N. Nudelman), gluck@newark.rutgers.edu (M.A. Gluck).
[1] 0000-0003-0552-8464
[2] 0000-0002-8412-1023
[3] 0009-0002-7858-5881
[4] 0009-0006-8579-711X
[5] 0009-0000-5988-7425
[6] 0000-0002-6314-4074
[7] 0000-0003-4040-1717
[8] 0000-0003-0538-2303

https://doi.org/10.1016/j.neurobiolaging.2026.01.008
Received 12 September 2025; Received in revised form 28 January 2026; Accepted 30 January 2026
Available online 1 February 2026
0197-4580/© 2026 Published by Elsevier Inc.

underlying early vulnerability remain understudied (Mayeda et al., 2016).

The medial temporal lobe (MTL), comprising memory-critical structures such as the hippocampus, entorhinal cortex, and perirhinal cortex, is among the earliest affected regions in AD (Berron et al., 2020). Although resting-state functional Magnetic Resonance Imaging (rs-fMRI) has provided key insights into large-scale brain network alterations in AD, static connectivity approaches overlook the brain's capacity for dynamic reconfiguration over short time periods (Hutchison et al., 2013). Dynamic functional connectivity, the brain's capacity to dynamically reconfigure connectivity (hereafter "flexibility"), quantifies transient shifts in connectivity states and is emerging as a sensitive marker of early neural dysfunction (McLaren et al., 2014). In the MTL, subtle disruptions in dynamic flexibility may reflect synaptic inefficiencies and early compensatory breakdowns that occur before structural atrophy (Dickerson and Sperling, 2008). Regional hyperactivity, inter-network hypo-connectivity, and instability in the MTL, have also been linked to impaired neuroplasticity and cognitive function (Dickerson et al., 2009; Dickerson and Sperling, 2008).

Genetic factors are a major contributor to AD, accounting for an estimated 58–79 % of disease risk at the population level (Mayeux, 2006). In African ancestry, two key genetic contributors to the late-onset AD are apolipoprotein E *(APOE)* and ATP-binding cassette subfamily A member 7 *(ABCA7)* (Stepler et al., 2022). While *APOE-ε4* allele is prevalent in this population, its associated risk is attenuated compared to European or Asian ancestry (Rajabli et al., 2018). The *APOE-ε4* allele is also associated with hippocampal hyperactivation in older African Americans (Sinha et al., 2018). On the other hand, *ABCA7 rs115550680* contributes to AD through the suppression of microglial *Aβ* clearance and is associated with AD development in African Americans (Aikawa et al., 2018; Stepler et al., 2022). The mechanistic underpinnings of ABCA7-related AD vulnerability still remain unclear, but prior evidence implicates its role in lipid metabolism, amyloid processing, and microglial function, all of which contribute to AD pathophysiology (Miao et al., 2023). Our prior work showed that *ABCA7 rs115550680* risk allele carriers had a functionally segregated entorhinal cortex and impaired learning, pointing to MTL network dysfunction as a potential early biomarker among older African Americans (Sinha et al., 2019).

The *ABCA7 rs115550680* risk allele exerts a stronger association with AD risk than the *APOE-ε4* allele in African Americans (De Roeck et al., 2019; Reitz et al., 2013; Stepler et al., 2022). We hypothesized that "*Cognitively unimpaired older African Americans carrying the ABCA7 rs115550680 risk alleles will exhibit reduced MTL flexibility and subregional hypertrophy compared to both non-carriers as well as to APOE-ε4 allele carriers, reflecting early neural dysfunction associated with preclinical AD*". The present study investigated the impact of *APOE-ε4* allele and *ABCA7 rs115550680* risk allele on flexibility and volume within the MTL region among cognitively unimpaired older African Americans. These findings aim to provide insights into ancestry-specific AD vulnerabilities which may inform future personalized-medicine targeted early intervention strategies.

2. Methods

2.1. Participants

Participants were recruited from an ongoing longitudinal study at Rutgers University–Newark of aging and AD risk in African Americans. Recruitment utilized the *Aging & Brain Health Alliance*, a university-community partnership engaging local senior centers, public and subsidized housing associations, religious institutions, health and wellness organizations, and other entities focused on the well-being of greater Newark residents. Recruitment through community-based outreach may preferentially attract individuals who are more health-engaged or who have personal or family concerns about cognitive aging, which may influence sample composition. All participants were distinct, unrelated individuals, and no relatives were included in the study.

Participants aged 60 years or older with a Mini-Mental State Examination (MMSE) score of 24 or above were eligible for inclusion for the current study. African American race/ethnicity was determined by participant self-report at enrollment. Exclusion criteria included any diagnosis of neurodegenerative disease, use of medications typically prescribed for dementia, history of learning disabilities, self-reported alcohol and/or drug abuse, general anesthesia within the past three months, MRI contraindications, and/or refusal to provide a saliva and/or blood sample. The study was approved by the Rutgers University Institutional Review Board, adhering to ethical guidelines and regulations of the Declaration of Helsinki.

2.2. Procedure

Potential participants received a telephone screening to assess initial eligibility. Those who met the criteria proceeded to provide informed consent. Subsequently, participants underwent a comprehensive laboratory visit including cognitive assessments, saliva collection, and MRI scans. All imaging and clinical data, including MRI and MMSE, were collected during the same study visit, and participant age in years reflects age at that visit.

2.3. Measures

2.3.1. Genetic procedures

Saliva samples for DNA extraction and genotyping were collected using DNA Genotek® Oragene (ORG-600) kits. These saliva sample tubes were securely stored in the laboratory before being processed for data analyses. Biosafety-trained research staff transported the samples to an off-site biotechnology facility for genotyping. The genotyping process involved quantitative PCR on Eppendorf Master cyclers using the TaqMan custom genotyping assay. Following genotyping, participants were classified as either *APOE-ε4* allele carriers or non-carriers, regardless of hetero- or homozygosity(Foster et al., 2017). All *APOE-ε4* allele heterozygotes were included in the study, even those with ε2/ε4 genotype, as the presence of the ε4 allele alone confers an increased risk for AD(Liu et al., 2013). *ABCA7 rs115550680* genotyping was performed using a quantitative polymerase chain reaction, identifying "G" allele carriers as *ABCA7 rs115550680* risk allele carriers(De Roeck et al., 2019). Genotyping was limited to selected candidate loci using TaqMan assays; genome-wide genotype data were not available.

2.3.2. MRI data acquisition

Participants underwent MRI at the Rutgers University Brain Imaging Center (RUBIC) located at the Rutgers University-Newark campus. MRI acquisitions were conducted through 3 T Siemens TRIO scanner equipped with a 32-channel multiband parallel encoding coil. Structural scans were performed with high-resolution 3D magnetization-prepared rapid gradient echo (MP-RAGE) in the sagittal plane (TR=1900ms, TE=2.52ms, 1.0 × 1.0 × 1.2 mm voxels). The scanning parameters for the high-resolution multiband echo-planar functional imaging (rs-fMRI) were as follows: TR= 664ms, 1.8 mm isotropic voxels, 812 time points, multiband factor= 5. Total acquisition time was ~14 min.

2.3.3. Resting state fMRI data analysis

2.3.3.1. Preprocessing. All neuroimaging data were processed and analyzed using AFNI (Linux) with standard afni_proc.py pipeline (Cox, 1996). Rs-fMRI data underwent despiking (3dDespike), slice timing correction (3dtshift), and alignment to skull-stripped MP-RAGE images (align_epi_anat.py). Motion was corrected (3dvolreg), and data were smoothed to 2 mm FWHM (3dmerge). A brain mask (3dautomask) excluded non-brain voxels. A custom script was implemented to ensure data integrity by excluding trials exhibiting motion exceeding 0.3 mm

from the time series, enhancing the reliability of the analyses. To reduce noise, ANATICOR was applied (Power et al., 2014). Nuisance regressors (six motion parameters and linear drift) were modeled with 3dDeconvolve. Structural scans were normalized via Advanced Normalization Tools (ANTs) employed a diffeomorphic nonlinear registration algorithm (SyN) to a custom 0.65 mm isotropic in-house template (Avants et al., 2008; Klein et al., 2009); aligned functional data were transformed to this template for group-level analysis.

2.3.3.2. Dynamic network construction. Dynamic functional connectivity within the MTL was investigated, focusing on cortical and hippocampal sub-regions (subiculum, Cornu Ammonis 1 (CA1), and Dentate Gyrus (DG)/CA3) as well as Perirhinal Cortex (PRC), Parahippocampal Cortex (PHC), Posteromedial Entorhinal Cortex (pMEC), and Anterolateral Entorhinal Cortex (aLEC). The PRC and PHC provide input respectively to the lateral and medial EC, which in turn project into the hippocampus. In this study, pMEC and aLEC were considered as separate ROIs within the MTL network. For each ROI (3dmaskave), an average time series encompassing 812 time points was extracted, excluding the initial six and last six time points. These time series were subsequently divided into sub-blocks of 50-time points (33 s) to evaluate the dynamic connectivity between ROIs across 16 time-windows. The duration of the time window was set to be long enough to allow for an accurate assessment of correlations throughout frequencies located in the wavelet band of interest (0.06–0.12 Hz), but short enough to allow for a fine-grained measurement of temporal evolution over the whole session (Telesford et al., 2016). For each of the 16 non-overlapping sub-blocks, connectivity was then determined as the magnitude squared spectral coherence between each pair of ROIs to quantify modularity across time frames (Bassett et al., 2013a, 2013b, 2011). Subject-specific $7 \times 7 \times 16$ connectivity matrices were constructed, representing coherence values ranging from 0 to 1 across 7 ROIs and 16 time-windows. Coherence, a measure of frequency-specific linear correlations between time series, was employed due to its efficacy in capturing functional relationships within the fMRI data (Sun et al., 2004). A multilayer network technique was employed, where each layer consists of a network derived from a single time window and subsequent layers correspond to subsequent time windows. This approach enabled the investigation of changes in functional brain network architecture over time. Each participant's multilayer networks were constructed by connecting nodes in the connectivity matrix to the equivalent node in the connectivity matrix of consecutive time windows. Networks were interconnected across time as a result of the multilayer network linking each network node to itself in previous and subsequent time slices. As a result of this representation, a time-dependent network was constructed that allows each network layer to be divided into densely interconnected sub-groups, called communities or modules, whose identities are reliably recorded over time frames (Bassett et al., 2013b; Mucha et al., 2010a).

2.3.3.3. Dynamic community detection. A Louvain-like locally greedy community detection algorithm for optimizing multilayer modularity was utilized to partition each multilayer network into temporally connected modules (Mucha et al., 2010b). A community assignment representing the module connectedness for each node and time frame was constructed by optimizing multilayer modularity. The flexibility of each node was defined as the extent to which it altered its module allegiance over the set of time frames represented by the multilayer network to enable it to measure alterations in the composition of communities through time (Bassett et al., 2013a, 2013b, 2011). Therefore, flexibility was calculated for each of our 7 ROIs (PRC, PHC, pMEC, aLEC, subiculum, CA1, DG/CA3) as the number of times a node indicated a change in community assignment, normalized by the total number of possible changes. The mean flexibility over all nodes was then computed to determine MTL dynamic network flexibility as the primary outcome. Overview of the rs-fMRI data preprocessing and dynamic network connectivity ("flexibility") analysis process was shown in Fig. 1a.

2.3.4. MTL subregional and anterior/posterior hippocampus segmentation and volume normalization

MTL subregions and anterior/posterior hippocampus were segmented using the Automatic Segmentation of Hippocampal Subfields (ASHS) toolbox (Xie et al., 2016), which uses high-resolution T1 -weighted structural MRI with multi-atlas label fusion to delineate distinct MTL structures. Segmented regions included the anterior and posterior hippocampus, ERC, Brodmann areas 35 and 36 (BA 35 and BA 36), and the PHC, bilaterally. To adjust for individual differences in head size, regional volumes were normalized to estimated total intracranial volume (eTIV) derived from FreeSurfer7.3.2 (Buckner et al., 2004; Fischl, 2012), using each participant's T1-weighted image. A representative example of the ASHS segmentation outputs is shown in Fig. 1b, illustrating the 3D reconstructions and coronal/sagittal overlays of the hippocampal and surrounding MTL subregions.

2.4. Statistical analysis

Jamovi version 2.6.24.0 was used for statistical analysis. Summary statistics and histograms were generated to evaluate data distributions, and outliers were checked. Statistical approaches that allow inclusion of cases with missing data were applied to maximize available information. No data were imputed; missing values were handled using model-wise exclusion such that participants were included in all analyses for which complete data were available. A series of general linear models (ANCOVAs) was conducted to examine group differences in the MTL flexibility and subregion volumes for

1) *ABCA7 rs115550680* risk allele carriers and non-carriers;
2) *APOE-ε4* allele carriers and non-carriers; and
3) Direct comparison of *ABCA7 rs115550680* risk allele-*only* carriers and *APOE-ε4 allele-only* carriers (excluding dual carriers).

All models included age, sex, and education as covariates; when *ABCA7 rs115550680* was the predictor, *APOE-ε4* status was additionally included as a covariate (and vice versa). APOE genotype was coded dichotomously as ε4 carrier versus non-carriers, with individuals carrying at least one ε4 allele (ε2/ε4, ε3/ε4, or ε4/ε4) classified as *APOE-ε4* allele carriers and all other genotypes classified as non-carriers. Critically, we also run two-way ANCOVA with factors *ABCA7 rs115550680* (risk allele carriers vs non-carriers) × *APOE-ε4* (allele carriers vs non-carriers) to test interaction effects on each outcome (covariates: age, sex, and education). MMSE was not included as a covariate because all participants were cognitively unimpaired, MMSE scores showed limited variability, and MMSE did not differ across genetic groups. Volumes were normalized to eTIV; therefore, eTIV was not added as a covariate. Results are reported as F, p, and partial η^2 (η_p^2) with $\alpha = .05$ (two-tailed). The significance value was accepted as $p < .05$.

3. Results

Demographics of the 146 participants (110 women) are shown in Table 1. Participants were between 60 and 90 years of age and on average had completed an associate degree or some college coursework. All participants were cognitively unimpaired. While 15.8 % of the participants were *ABCA7 rs115550680* risk allele carriers, 43.8 % of them were *APOE-ε4* allele carriers. Of 23 ABCA7 *rs115550680* risk allele carriers, 9 (39 %) were also *APOE-ε4* allele carriers; among *ABCA7 rs115550680* non-carriers (n = 123), 55 were *APOE-ε4* allele carriers and 68 were non-carriers. The joint distribution of *ABCA7 rs115550680* and *APOE-ε4* carrier status is shown in Supplementary Table 1. Demographic and clinical characteristics, including age, sex, education, and MMSE, did not differ significantly across genetic groups (Supplementary Table 1).

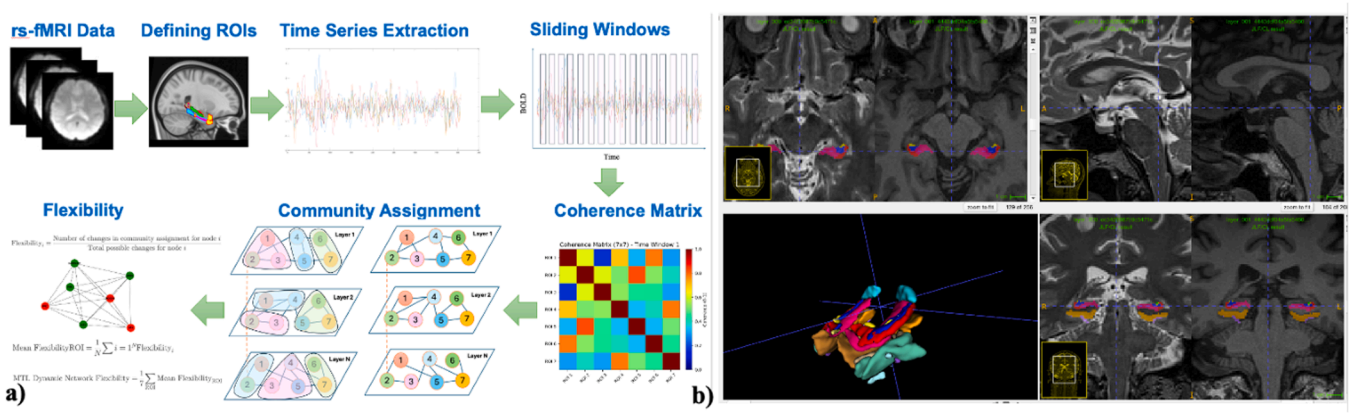

Fig. 1. a) Overview of rs-fMRI Preprocessing and Dynamic Network Analysis Pipeline. This diagram illustrates the fMRI preprocessing steps and dynamic functional connectivity analysis workflow. Steps include anatomical registration, motion correction, signal regression, and transformation to template space using ANTs. Dynamic connectivity was estimated across 16-time windows using coherence and multilayer modularity. Flexibility was computed from changes in community structure over time across seven medial temporal lobe (MTL) regions of interest. Abbreviations: ANTs = Advanced Normalization Tools; MTL = medial temporal lobe. b) Segmentation of Hippocampal Subfields and Medial Temporal Lobe Subregions. Example segmentation of MTL subregions using ASHS. Coronal and sagittal views show bilateral delineation of the entorhinal cortex, parahippocampal cortex, and hippocampal subfields (including anterior and posterior hippocampus, Brodmann areas 35 and 36). The bottom left panel displays a 3D rendering of the segmented MTL structures. Abbreviations: ASHS = Automatic Segmentation of Hippocampal Subfields; MTL = medial temporal lobe.

Table 1
Distribution of demographic data and volumes.

Demographics		Mean ± SD
Age (years of age) (Mean ± SD)		69.71 ± 6.29
Sex (N (%))	Woman	110 (75.4)
	Man	36 (24.7)
Education (years) (Mean ± SD)		14.71 ± 5.52
MMSE (Mean ± SD)		27.80 ± 1.90
ABCA7 rs115550680 (N (%))	High-Risk Allele Carriers	23 (15.8)
	Non-Risk Allele Carriers	123 (84.2)
APOE-ε4 (N (%))	High-Risk Allele Carriers	64 (43.8)
	Non-Risk Allele Carriers	82 (56.2)
	ε2ε2 Allele Carriers	2 (1.4)
	ε2ε3 Allele Carriers	13 (8.9)
APOE Genotype (N (%))	ε3ε3 Allele Carriers	67 (45.9)
	ε2ε4 Allele Carriers	10 (6.8)
	ε3ε4 Allele Carriers	51 (34.9)
	ε4ε4 Allele Carriers	3 (2.1)
Volumes		Mean ± SD
Estimated Total Intracranial Volume		1,361,030 ± 148,006
Anterior Hippocampus*	Right Hemisphere	1.12 ± 0.16
	Left Hemisphere	1.03 ± 0.13
Posterior Hippocampus*	Right Hemisphere	1.14 ± 0.16
	Left Hemisphere	1.18 ± 0.14
ERC*	Right Hemisphere	0.35 ± 0.05
	Left Hemisphere	0.36 ± 0.05
BA35*	Right Hemisphere	0.39 ± 0.10
	Left Hemisphere	0.38 ± 0.06
BA36*	Right Hemisphere	1.15 ± 0.19
	Left Hemisphere	1.25 ± 0.19
PHC*	Right Hemisphere	0.65 ± 0.11
	Left Hemisphere	0.65 ± 0.11

Note. MMSE = Mini-Mental State Examination; SD = standard deviation; N = number; % = percentage; MTL = medial temporal lobe; ERC = entorhinal cortex; BA = Brodmann area; PHC = parahippocampal cortex. *Volumes were normalized to estimated total intracranial volume.*

3.1. Main and interaction effects of ABCA7 rs115550680 and APOE-ε4 genotype

ABCA7 rs115550680 risk allele carriers exhibited significantly lower MTL flexibility compared to non-carriers ($F_{(1140)}$= *4.200,* $\eta\rho^2$= *.029,* p = *.042*) with an observed power of 0.530 (Fig. 2a). There was no statistically significant impact of *APOE-ε4* allele on MTL flexibility ($F_{(1141)}$= *2.043,*$\eta\rho^2$= *.014,*p = *.155*) with an observed power of 0.295. *ABCA7 rs115550680* risk allele carriers demonstrated significant hypertrophy in left anterior hippocampus ($F_{(1140)}$= *3.934,*$\eta\rho^2$= *.027,* p = *.049*), left ERC ($F_{(1140)}$= *5.500,*$\eta\rho^2$= *.037,*p = *.020*), right ERC ($F_{(1140)}$= *3.981,*$\eta\rho^2$= *.026,*p = *.048*), and marginal difference in right anterior hippocampus ($F_{(1140)}$= *3.808,*$\eta\rho^2$= *.026,*p = *.053*) compared to non-carriers (Table 2). There was no difference in the MTL subregional volumes between *APOE-ε4* allele carriers and non-carriers ($p > .05$). Across outcomes, the *ABCA7 rs115550680* × *APOE-ε4* interaction was not significant for MTL flexibility or MTL subregional volumes (all $p > .05$). (Supplementary Table 3).

3.2. Difference between ABCA7 rs115550680 risk allele-only and APOE-ε4 allele-only carriers

Of 23 *ABCA7 rs115550680* risk allele carriers, 9 (39 %) also carried *APOE-ε4* allele and were excluded from the direct comparisons. Among *ABCA7 rs115550680* non-carriers (n = 123), 55 were *APOE-ε4* allele carriers and 68 were non-carriers. Direct comparisons therefore focused on *ABCA7 rs115550680* risk allele–only carriers versus *APOE-ε4* allele–only carriers, excluding individuals carrying both risk alleles.

ABCA7 rs115550680 risk allele-only carriers demonstrated significantly lower MTL flexibility ($F_{(1,64)}$= *4.924,* $\eta\rho^2$= *.069,* p = *.030*) with an observed power of 0.590 than *APOE-ε4* allele-only carriers (Fig. 2b). *ABCA7 rs115550680* risk allele-only carriers showed significant hypertrophy in left ERC compared to *APOE-ε4* allele-only carriers ($F_{(1,64)}$ = 5.137, η_p^2 = .072, p = .027) (Table 3).

4. Discussion

In this study, *ABCA7 rs115550680* risk allele carriers exhibited significantly reduced MTL flexibility compared to both non-carriers and *APOE-ε4* allele carriers. They also showed hypertrophy in the left anterior hippocampus and bilateral ERC. Taken together, these findings suggest preliminary evidence that *ABCA7 rs115550680* risk allele may uniquely capture early MTL network dysfunction in older African Americans. The observed subregional volumes could reflect transient, possibly compensatory or inflammatory, remodeling in MTL subregions rather than stable structural change. Overall, these findings support that

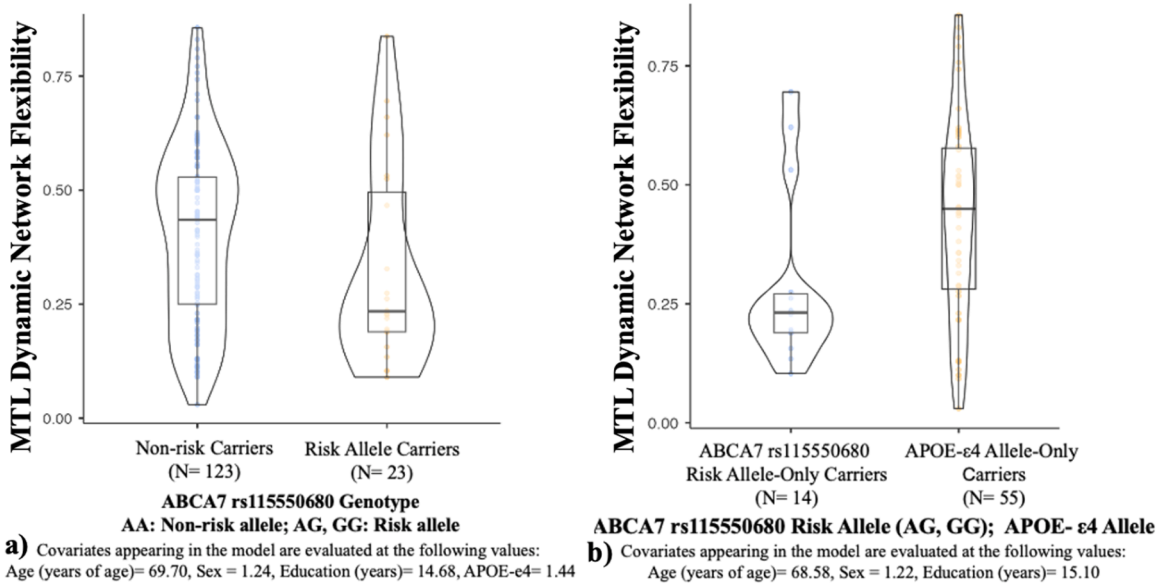

Fig. 2. a) Reduced Medial Temporal Lobe Flexibility in *ABCA7 rs115550680* Risk Allele Carriers. Violin plots show the distribution of MTL dynamic network flexibility values for ABCA7 *rs115550680* risk allele carriers (AG, GG) and non-carriers (AA). Each plot illustrates the full range, kernel density estimate, and median (horizontal line) within each group. Group comparisons were adjusted for age, sex, and education. Abbreviation: MTL = medial temporal lobe. b) *ABCA7 rs115550680* Risk Allele Carriers Show Lower MTL Flexibility than *APOE-ε4* Allele Carriers. Violin plots compare MTL dynamic network flexibility between individuals with only the *ABCA7 rs115550680* risk allele-only (N = 14) and those carrying *APOE-ε4* allele-only (N = 55). Each plot shows the distribution, kernel density, and median flexibility values. Statistical models were adjusted for age, sex, and education. Abbreviations: MTL = medial temporal lobe; APOE = apolipoprotein E.

Table 2
Main effect of *ABCA7 rs115550680* and *APOE-ε4* genotype.

ABCA7 rs115550680		Risk Allele Carriers(N = 23)	Non-Carriers(N = 123)	Statistics
		Mean ± SD	Mean ± SD	
Estimated Total Intracranial Volume		1357,654 ± 160,974	1363,665 ± 379,989	$F_{(1140)} = .106$, $\eta_p^2 = .001$, $p = .745$
Anterior Hippocampus*	Right Hemisphere	1.11 ± 0.18	1.12 ± 0.15	$F_{(1140)} = 3.808$, $\eta_p^2 = .026$, $p = .053$
	Left Hemisphere	1.03 ± 0.14	1.03 ± 0.13	$F_{(1140)} = 3.934$, $\eta_p^2 = .027$, $\mathbf{p = .049}$
Posterior Hippocampus*	Right Hemisphere	1.14 ± 0.19	1.14 ± 0.12	$F_{(1140)} = .185$, $\eta_p^2 = .001$, $p = .668$
	Left Hemisphere	1.19 ± 0.16	1.18 ± 0.12	$F_{(1140)} = .264$, $\eta_p^2 = .002$, $p = .608$
ERC*	Right Hemisphere	0.35 ± 0.05	0.36 ± 0.05	$F_{(1140)} = 3.981$, $\eta_p^2 = .027$, $\mathbf{p = .048}$
	Left Hemisphere	0.35 ± 0.05	0.36 ± 0.05	$F_{(1140)} = 5.500$, $\eta_p^2 = .037$, $\mathbf{p = .020}$
BA35*	Right Hemisphere	0.40 ± 0.13	0.38 ± 0.06	$F_{(1140)} = .575$, $\eta_p^2 = .004$, $p = .449$
	Left Hemisphere	0.37 ± 0.06	0.38 ± 0.06	$F_{(1140)} = .003$, $\eta_p^2 = .000$, $p = .953$
BA36*	Right Hemisphere	1.13 ± 0.21	1.16 ± 0.16	$F_{(1140)} = .668$, $\eta_p^2 = .005$, $p = .415$
	Left Hemisphere	1.21 ± 0.17	1.27 ± 0.19	$F_{(1140)} = .157$, $\eta_p^2 = .001$, $p = .692$
PHC*	Right Hemisphere	0.65 ± 0.11	0.65 ± 0.11	$F_{(1140)} = .478$, $\eta_p^2 = .003$, $p = .491$
	Left Hemisphere	0.66 ± 0.12	0.65 ± 0.11	$F_{(1140)} = .315$, $\eta_p^2 = .002$, $p = .576$
APOE-ε4		ε4 Allele Carriers(N = 64)	Non-Carriers(N = 82)	Statistics
		Mean ± SD	Mean ± SD	
Estimated Total Intracranial Volume		1349,124 ± 163,112	1366,422 ± 138,872	$F_{(1141)} = .046$, $\eta_p^2 = .000$, $p = .830$
Anterior Hippocampus*	Right Hemisphere	1.12 ± 0.17	1.12 ± 0.15	$F_{(1141)} = .191$, $\eta_p^2 = .001$, $p = .663$
	Left Hemisphere	1.03 ± 0.13	1.03 ± 0.14	$F_{(1141)} = .039$, $\eta_p^2 = .000$, $p = .844$
Posterior Hippocampus*	Right Hemisphere	1.14 ± 0.16	1.14 ± 0.12	$F_{(1141)} = .000$, $\eta_p^2 = .000$, $p = .990$
	Left Hemisphere	1.18 ± 0.15	1.18 ± 0.11	$F_{(1141)} = .091$, $\eta_p^2 = .001$, $p = .764$
ERC*	Right Hemisphere	0.35 ± 0.04	0.35 ± 0.05	$F_{(1141)} = 1.129$, $\eta_p^2 = .008$, $p = .290$
	Left Hemisphere	0.36 ± 0.05	0.36 ± 0.05	$F_{(1141)} = 2.601$, $\eta_p^2 = .018$, $p = .109$
BA35*	Right Hemisphere	0.38 ± 0.06	0.38 ± 0.06	$F_{(1141)} = .802$, $\eta_p^2 = .006$, $p = .372$
	Left Hemisphere	0.37 ± 0.06	0.38 ± 0.06	$F_{(1141)} = .947$, $\eta_p^2 = .007$, $p = .332$
BA36*	Right Hemisphere	1.14 ± 0.18	1.16 ± 0.17	$F_{(1141)} = 1.144$, $\eta_p^2 = .008$, $p = .287$
	Left Hemisphere	1.25 ± 0.18	1.27 ± 0.20	$F_{(1141)} = 3.774$, $\eta_p^2 = .026$, $p = .054$
PHC*	Right Hemisphere	0.65 ± 0.12	0.65 ± 0.11	$F_{(1141)} = .034$, $\eta_p^2 = .000$, $p = .854$
	Left Hemisphere	0.66 ± 0.11	0.65 ± 0.11	$F_{(1141)} = .029$, $\eta_p^2 = .000$, $p = .866$

Note. SD = standard deviation; MTL = medial temporal lobe; ERC = entorhinal cortex; BA = Brodmann area; PHC = parahippocampal cortex. *Volumes were normalized to estimated total intracranial volume.*

MTL flexibility may reflect early neural alterations associated with AD risk among older African Americans.

Neuroimaging plays a pivotal role in detecting early AD-related brain changes. The MTL, including the hippocampus and ERC, is among the earliest regions affected, often before cognitive symptoms emerge. Functional connectivity disruptions, particularly hyperconnectivity in MTL, has been reported in early AD (Nakamura et al., 2017) and may precede structural atrophy (Das et al., 2013; Duchateau et al., 2024).

Table 3
Comparison between *ABCA7 rs115550680* risk allele-only carriers and *APOE-ε4* allele–only carriers.

		ABCA7 rs115550680–Risk Allele-Only Carriers (N = 14)	*APOE-ε4 Allele–Only Carriers* (N = 55)	Statistics
		Mean ± SD	Mean ± SD	
Estimated Total Intracranial Volume		1363,664 ± 135,006	1354,861 ± 158,740	$F_{(1,67)} = .035$, $\eta_p^2 = .001$, $p = .852$
Anterior Hippocampus*	Right Hemisphere	1.14 ± 0.20	1.09 ± 0.17	$F_{(1,67)} = .796$, $\eta_p^2 = .012$, $p = .376$
	Left Hemisphere	1.06 ± 0.14	1.01 ± 0.14	$F_{(1,67)} = 1.196$, $\eta_p^2 = .018$, $p = .278$
Posterior Hippocampus*	Right Hemisphere	1.17 ± 0.13	1.15 ± 0.21	$F_{(1,67)} = .165$, $\eta_p^2 = .002$, $p = .686$
	Left Hemisphere	1.23 ± 0.17	1.20 ± 0.16	$F_{(1,67)} = .382$, $\eta_p^2 = .006$, $p = .539$
ERC*	Right Hemisphere	0.36 ± 0.06	0.34 ± 0.05	$F_{(1,67)} = 1.687$, $\eta_p^2 = .025$, $p = .199$
	Left Hemisphere	0.38 ± 0.06	0.34 ± 0.05	$F_{(1,67)} = 5.137$, $\eta_p^2 = .072$, $\mathbf{p = .027}$
BA35*	Right Hemisphere	0.36 ± 0.08	0.40 ± 0.14	$F_{(1,67)} = .774$, $\eta_p^2 = .012$, $p = .382$
	Left Hemisphere	0.38 ± 0.07	0.37 ± 0.07	$F_{(1,67)} = .280$, $\eta_p^2 = .004$, $p = .599$
BA36*	Right Hemisphere	1.15 ± 0.17	1.14 ± 0.22	$F_{(1,67)} = .017$, $\eta_p^2 = .000$, $p = .897$
	Left Hemisphere	1.30 ± 0.24	1.21 ± 0.18	$F_{(1,67)} = 2.106$, $\eta_p^2 = .031$, $p = .151$
PHC*	Right Hemisphere	0.66 ± 0.12	0.64 ± 0.12	$F_{(1,67)} = .195$, $\eta_p^2 = .003$, $p = .660$
	Left Hemisphere	0.69 ± 0.15	0.66 ± 0.12	$F_{(1,67)} = .465$, $\eta_p^2 = .007$, $p = .498$

Note. SD = standard deviation; MTL = medial temporal lobe; ERC = entorhinal cortex; BA = Brodmann area; PHC = parahippocampal cortex. *Volumes were normalized to estimated total intracranial volume.*

Our study builds on this by leveraging dynamic flexibility, a more sensitive measure of neural dysfunction compared to static approaches (Hutchison et al., 2013). Altered MTL flexibility may reflect synaptic inefficiencies and early network breakdowns (Sperling et al., 2010).

Our results show that carriers of the *ABCA7 rs115550680* risk allele exhibited significantly reduced dynamic network flexibility within the MTL region compared with non-carriers. This finding is particularly relevant given that ABCA7 is involved in lipid metabolism, amyloid processing, and microglial function, all of which are implicated in AD pathophysiology (Aikawa et al., 2018; Dib et al., 2021; Duchateau et al., 2024). The *ABCA7 rs115550680* risk allele, which is associated with impaired Aβ clearance and defective microglial response, may lead to early disruptions in MTL network dynamics, thereby compromising the brain's ability to engage in efficient communication across networks. These findings highlight the utility of dynamic network flexibility as a sensitive biomarker capable of detecting subtle genetic effects on MTL function.

Notably, we also observed subregional hypertrophy—an increase in tissue volume due to enlargement of cellular components—in *ABCA7 rs115550680* risk allele carriers, including the left anterior hippocampus and bilateral ERC, compared to non-carriers. Such hypertrophy may represent a transient, possibly compensatory or inflammatory response, consistent with prior reports linking astrocytic reactivity to early volumetric expansion before subsequent atrophy. These results are consistent with earlier studies that suggest *ABCA7* plays a more significant role in AD risk among individuals of African ancestry although not in those of primarily European ancestry (Berg et al., 2019; Reitz et al., 2013; Sinha et al., 2019; Stepler et al., 2022). Given that the *ABCA7 rs115550680* risk allele has been linked in our own prior studies to a functionally segregated ERC, this dysfunction may manifest as deficits in prior learning, as we observed in our cohort (Berg et al., 2019; De Roeck et al., 2019; Sinha et al., 2019; Stepler et al., 2022). Although our structural analyses were limited to anterior/posterior hippocampal divisions, the expression of ABCA7 in the CA1 region raises the possibility that subfield-specific vulnerability may underlie some of the observed network alteration (Rosenthal and Kamboh, 2014). Understanding whether these structural alterations represent compensatory resilience or a precursor to decline will be critical for developing ancestry-informed biomarkers of AD risk.

Functional alterations in MTL flexibility may reflect early neural alterations associated with AD risk among older African Americans, possibly preceding detectable atrophy in some regions while co-occurring with compensatory-driven expansion in others. In contrast, the *APOE-ε4* allele did not demonstrate a significant effect on MTL dynamic network flexibility in our study. Although *APOE-ε4* allele remains one of the most robust genetic risk factors for AD in individuals of European descent, its role in AD pathology among individuals of African ancestry has been less well characterized. While previous research has linked *APOE-ε4* allele to hippocampal hyperactivation and prior learning deficits in this population (Barnes and Bennett, 2014; Murrell et al., 2006; Saeed et al., 2018; Sinha et al., 2018), our findings suggest that influence of *APOE-ε4* allele on MTL network dynamics may be weaker or more subtle than previously assumed. Future studies integrating multimodal imaging and ancestry-informative genetic markers will be important to disentangle the nuanced effects of *APOE-ε4* on neural network organization in this population.

When comparing the effects of "*ABCA7 rs115550680* risk allele-only" and "*APOE-ε4* allele-only" *and* "*ABCA7 rs115550680* x *APOE-ε4*" interaction model, our results reveal that *ABCA7 rs115550680 risk allele-only* carriers exhibit significantly lower MTL dynamic network flexibility than *APOE-ε4* allele-only carriers and no effect on interaction model. Additionally, *ABCA7 rs115550680 risk allele-only* carriers demonstrated significant hypertrophy in the left ERC compared to *APOE-ε4* allele-only carriers, suggesting the possibility of subregional structural remodeling, potentially driven by early compensatory functions. These findings highlight the potentially stronger influence of *ABCA7 rs115550680* risk allele on early neural dysfunction in African ancestry, underscoring its significance as a genetic risk factor for AD in this population. Taken together, these results highlight that *ABCA7 rs115550680* risk allele may exert a comparatively stronger influence on MTL flexibility than *APOE-ε4* allele in African Americans, though replication in independent cohorts is required.

Previous studies have demonstrated that the risk conferred by *APOE-ε4* allele varies across populations and is influenced by local ancestry at the APOE locus. Recent evidence also suggests that an African-origin haplotype within the APOE region may confer protection against AD

among *APOE-ε4* allele carriers (Nasciben et al., 2025). Together, these findings emphasize that the impact of genetic risk factors such as *APOE-ε4* and *ABCA7 rs115550680* can differ depending on ancestry background, highlighting the importance of considering local ancestry in genetic studies of AD. Our findings are consistent with previous reports that suggest *ABCA7 rs115550680* risk allele may exert a stronger influence than *APOE-ε4* allele in individuals of African ancestry (Reitz et al., 2013). By demonstrating the greater impact of ABCA7 *rs115550680* risk allele on MTL dynamic network flexibility, along with structural distinctions, our study emphasizes the need for a nuanced understanding of population-specific genetic vulnerabilities to AD.

Several limitations should be considered when interpreting these findings. *First,* the cross-sectional design limits causal inference and longitudinal studies are necessary to track changes in MTL network dynamics over time and examine how early disruptions in network flexibility may serve as predictive markers for the onset of cognitive decline and clinical AD. *Second,* the neuroimaging analysis focused solely on the MTL region, leaving open whether other brain regions show similar genetic effects. Future research to include broader brain networks could offer valuable insights into regional differences in the impact of genetic risk factors on neural network flexibility. In addition, our structural data were derived from T1-weighted imaging only, which limits the resolution needed to detect fine-grained subfield atrophy. Incorporating high-resolution T2-weighted imaging may improve sensitivity to early changes. *Third,* a relatively small sample size may have constrained the statistical power to detect subtle effects. Moreover, while we focused on genetic variants in *APOE-ε4* and *ABCA7 rs115550680*, other established genetic risk factors for AD were not considered. Future studies should aim to replicate these findings in larger, ancestrally diverse cohorts and explore polygenic influences on MTL network function across both structural and functional domains. *Fourth,* genetic analyses were restricted to a targeted panel of candidate variants. In particular, the functional 44–base-pair ABCA7 frameshift deletion (*rs142076058*), which has been implicated in AD risk among African ancestry populations, was not directly genotyped. Instead, the present study focused on *ABCA7 rs115550680*, a well-established variant that is in strong linkage disequilibrium with *rs142076058* in African ancestry individuals and is widely used as a tagging marker in prior studies (Berg et al., 2019; De Roeck et al., 2019; Del-Aguila et al., 2015; Dib et al., 2021; Duchateau et al., 2024; Li et al., 2015; Reitz et al., 2013). Future studies incorporating sequencing-based approaches or direct genotyping of structural ABCA7 variants will be important for clarifying underlying biological mechanisms. *Fifth,* because genome-wide genotype data were not available, population stratification could not be formally controlled using ancestry principal components. Although analyses were restricted to self-identified African American participants, residual within-group ancestry heterogeneity cannot be excluded and should be considered when interpreting the results. *Sixth,* participants were recruited through a community-engaged volunteer cohort, which may introduce self-selection bias, as individuals with heightened interest in brain health or a family history of dementia may be more likely to participate. In addition, the majority of participants were women, reflecting enrollment patterns commonly observed in community-based aging studies, which may limit generalizability to older African American men. *Finally,* given the exploratory and hypothesis-generating nature of this study, formal correction for multiple comparisons was not applied. Primary analyses were guided by a priori hypotheses focused on MTL network flexibility and selected MTL subregions based on prior literature (Brown et al., 2024; Chauveau et al., 2021; Das et al., 2013; Dickerson et al., 2009; Dickerson and Sperling, 2008; Hrybouski et al., 2023; Kang et al., 2024; Krasuski et al., 1998; Kukolja et al., 2010; Pasquini et al., 2016; Prieto et al., 2020; Sheldon and Levine, 2018; Soldan et al., 2015; Wolk et al., 2017). Accordingly, findings are interpreted cautiously as preliminary evidence, and replication in independent and longitudinal cohorts will be essential to confirm these associations.

In conclusion, our findings provide preliminary evidence that the *ABCA7 rs115550680* risk allele, but not APOE-*ε4 allele*, is associated with reduced MTL flexibility and subregional hypertrophy in cognitively unimpaired older African Americans. These results suggest that *ABCA7 rs115550680 risk allele* may exert a comparatively stronger influence on early neural dysfunction than *APOE-ε4* allele in this population. While the mechanisms remain to be clarified, the observed alterations could reflect transient, possibly compensatory or inflammatory remodeling processes. Importantly, our study underscores the need to consider ancestry-specific genetic risk factors when investigating early biomarkers of AD. Dynamic connectivity measures may offer a sensitive tool for detecting subtle genetic influences on brain function, but replication in larger, longitudinal, and ancestrally diverse cohorts will be critical to validate these observations and to inform strategies for early detection and precision-prevention in high-risk populations.

CRediT authorship contribution statement

Kelly N. Nudelman: Writing – review & editing, Supervision, Methodology. **Mark A. Gluck:** Writing – review & editing, Writing – original draft, Visualization, Supervision, Resources, Methodology, Funding acquisition, Conceptualization. **Soodeh Moallemian:** Writing – review & editing, Visualization, Methodology. **Miray Budak:** Writing – review & editing, Writing – original draft, Visualization, Validation, Resources, Methodology, Investigation, Formal analysis, Data curation, Conceptualization. **Payton White:** Writing – review & editing, Visualization, Methodology, Conceptualization. **Martina Ishaq:** Writing – review & editing, Formal analysis, Data curation. **Bernadette A. Fausto:** Writing – review & editing, Writing – original draft, Supervision, Methodology, Formal analysis, Conceptualization. **Victoria Paruzel:** Writing – original draft, Visualization, Methodology, Conceptualization.

Consent statement

All study participants provided written informed consent prior to enrollment in accordance with institutional guidelines approved by the Rutgers University Institutional Review Board.

Funding

This work was supported by the National Institutes of Health, National Institute on Aging [grant number 1R01AG053961]. The funding source had no role in the study design; in the collection, analysis, or interpretation of data; in the writing of the report; or in the decision to submit the article for publication.

Declaration of Competing Interest

The authors declare that they have no known competing financial interests or personal relationships that could have appeared to influence the work reported in this paper.

Acknowledgments

We are grateful for the feedback and shared insights from our Community Brain Health Educators and Outreach Team: Glenda Wright, Delores Hammonds, Jerome Perkins, Louches Powell, Reverend Glenn Wilson, and Catherine Willis. We are indebted to the thousands of community members who have participated in our brain health events since 2006, and to over 450 community members who have enrolled, to date, as VIPs (Very Important Participants) in our *Aging & Brain Health Alliance* study.

Appendix A. Supporting information

Supplementary data associated with this article can be found in the

online version at doi:10.1016/j.neurobiolaging.2026.01.008.

References

Aikawa, T., Holm, M.-L., Kanekiyo, T., Aikawa, T., Holm, M.-L., Kanekiyo, T., 2018. ABCA7 and pathogenic pathways of Alzheimer's disease. Brain Sci. 8. https://doi.org/10.3390/brainsci8020027.

Avants, B., Tustison, N., Song, G., 2008. Advanced normalization tools (ANTS). Insight J. 1–35. https://doi.org/10.54294/uvnhin.

Barnes, L.L., 2022. Alzheimer disease in African American individuals: increased incidence or not enough data? Nat. Rev. Neurol. 18, 56–62. https://doi.org/10.1038/s41582-021-00589-3.

Barnes, L.L., Bennett, D.A., 2014. Alzheimer's disease in African Americans: risk factors and challenges for the future. Health Aff. Proj. Hope 33, 580–586. https://doi.org/10.1377/hlthaff.2013.1353.

Bassett, D.S., Porter, M.A., Wymbs, N.F., Grafton, S.T., Carlson, J.M., Mucha, P.J., 2013a. Robust detection of dynamic community structure in networks. Chaos Woodbury N. 23, 013142. https://doi.org/10.1063/1.4790830.

Bassett, D.S., Wymbs, N.F., Porter, M.A., Mucha, P.J., Carlson, J.M., Grafton, S.T., 2011. Dynamic reconfiguration of human brain networks during learning. Proc. Natl. Acad. Sci. USA 108, 7641–7646. https://doi.org/10.1073/pnas.1018985108.

Bassett, D.S., Wymbs, N.F., Rombach, M.P., Porter, M.A., Mucha, P.J., Grafton, S.T., 2013b. Task-based core-periphery organization of human brain dynamics. PLOS Comput. Biol. 9, e1003171. https://doi.org/10.1371/journal.pcbi.1003171.

Berg, C.N., Sinha, N., Gluck, M.A., 2019. The effects of APOE and ABCA7 on cognitive function and Alzheimer's disease risk in African Americans: a focused mini review. Front. Hum. Neurosci. 13, 387. https://doi.org/10.3389/fnhum.2019.00387.

Berron, D., van Westen, D., Ossenkoppele, R., Strandberg, O., Hansson, O., 2020. Medial temporal lobe connectivity and its associations with cognition in early Alzheimer's disease. Brain 143, 1233–1248. https://doi.org/10.1093/brain/awaa068.

Brown, C., Das, S., Xie, L., Nasrallah, I., Detre, J., Chen-Plotkin, A., Shaw, L., McMillan, C., Yushkevich, P., Wolk, D., 2024. Medial temporal lobe gray matter microstructure in preclinical Alzheimer's disease. Alzheimers Dement 20, 4147–4158. https://doi.org/10.1002/alz.13832.

Buckner, R.L., Head, D., Parker, J., Fotenos, A.F., Marcus, D., Morris, J.C., Snyder, A.Z., 2004. A unified approach for morphometric and functional data analysis in young, old, and demented adults using automated atlas-based head size normalization: reliability and validation against manual measurement of total intracranial volume. NeuroImage 23, 724–738. https://doi.org/10.1016/j.neuroimage.2004.06.018.

Chauveau, L., Kuhn, E., Palix, C., Felisatti, F., Ourry, V., de La Sayette, V., Chételat, G., de Flores, R., 2021. Medial temporal lobe subregional atrophy in aging and Alzheimer's disease: a longitudinal study. Front. Aging Neurosci. 13, 750154. https://doi.org/10.3389/fnagi.2021.750154.

Cox, R.W., 1996. AFNI: software for analysis and visualization of functional magnetic resonance neuroimages. Comput. Biomed. Res. Int. J. 29, 162–173. https://doi.org/10.1006/cbmr.1996.0014.

Das, S.R., Pluta, J., Mancuso, L., Kliot, D., Orozco, S., Dickerson, B.C., Yushkevich, P.A., Wolk, D.A., 2013. Increased functional connectivity within medial temporal lobe in mild cognitive impairment. Hippocampus 23, 1–6. https://doi.org/10.1002/hipo.22051.

De Roeck, A., Van Broeckhoven, C., Sleegers, K., 2019. The role of ABCA7 in Alzheimer's disease: evidence from genomics, transcriptomics and methylomics. Acta Neuropathol. (Berl.) 138, 201–220. https://doi.org/10.1007/s00401-019-01994-1.

Del-Aguila, J.L., Fernández, M.V., Jimenez, J., Black, K., Ma, S., Deming, Y., Carrell, D., Saef, B., Howells, B., Budde, J., Cruchaga, C., Alzheimer's Disease Neuroimaging Initiative, 2015. Role of ABCA7 loss-of-function variant in Alzheimer's disease: a replication study in European–Americans. Alzheimers Res. Ther. 7, 73. https://doi.org/10.1186/s13195-015-0154-x.

Dib, S., Pahnke, J., Gosselet, F., 2021. Role of ABCA7 in Human Health and in Alzheimer's Disease. Int. J. Mol. Sci. 22, 4603. https://doi.org/10.3390/ijms22094603.

Dickerson, B.C., Feczko, E., Augustinack, J.C., Pacheco, J., Morris, J.C., Fischl, B., Buckner, R.L., 2009. Differential effects of aging and Alzheimer's disease on medial temporal lobe cortical thickness and surface area. Neurobiol. Aging 30, 432–440. https://doi.org/10.1016/j.neurobiolaging.2007.07.022.

Dickerson, B.C., Sperling, R.A., 2008. Functional abnormalities of the medial temporal lobe memory system in mild cognitive impairment and Alzheimer's disease: insights from functional MRI studies. Neuropsychol. Neuroimaging Early Alzheimer'S. Dis. 46, 1624–1635. https://doi.org/10.1016/j.neuropsychologia.2007.11.030.

Duchateau, L., Wawrzyniak, N., Sleegers, K., 2024. The ABC's of Alzheimer risk gene ABCA7 (n/a). Alzheimers Dement. https://doi.org/10.1002/alz.13805.

Fischl, B., 2012. FreeSurfer. NeuroImage 20 YEARS fMRI 62, 774–781. https://doi.org/10.1016/j.neuroimage.2012.01.021.

Foster, C.M., Kennedy, K.M., Rodrigue, K.M., 2017. Differential aging trajectories of modulation of activation to cognitive challenge in APOE ε4 groups: reduced modulation predicts poorer cognitive performance. J. Neurosci. 37, 6894–6901. https://doi.org/10.1523/JNEUROSCI.3900-16.2017.

Hrybouski, S., Das, S.R., Xie, L., Wisse, L.E.M., Kelley, M., Lane, J., Sherin, M., DiCalogero, M., Nasrallah, I., Detre, J., Yushkevich, P.A., Wolk, D.A., 2023. Aging and Alzheimer's disease have dissociable effects on local and regional medial temporal lobe connectivity. Brain Commun. 5, fcad245. https://doi.org/10.1093/braincomms/fcad245.

Hutchison, R.M., Womelsdorf, T., Allen, E.A., Bandettini, P.A., Calhoun, V.D., Corbetta, M., Penna, S.D., Duyn, J.H., Glover, G.H., Gonzalez-Castillo, J., Handwerker, D.A., Keilholz, S., Kiviniemi, V., Leopold, D.A., de Pasquale, F., Sporns, O., Walter, M., Chang, C., 2013. Dynamic functional connectivity: Promise, issues, and interpretations, 10.1016/j.neuroimage.2013.05.079 NeuroImage 80. https://doi.org/10.1016/j.neuroimage.2013.05.079.

Kang, S., Jeon, S., Lee, Y., Ye, B.S., 2024. Alteration of medial temporal lobe metabolism related to Alzheimer's disease and dementia with lewy bodies. Alzheimers Res. Ther. 16, 89. https://doi.org/10.1186/s13195-024-01429-4.

Klein, A., Andersson, J., Ardekani, B.A., Ashburner, J., Avants, B., Chiang, M.-C., Christensen, G.E., Collins, D.L., Gee, J., Hellier, P., Song, J.H., Jenkinson, M., Lepage, C., Rueckert, D., Thompson, P., Vercauteren, T., Woods, R.P., Mann, J.J., Parsey, R.V., 2009. Evaluation of 14 nonlinear deformation algorithms applied to human brain MRI registration. NeuroImage 46, 786–802. https://doi.org/10.1016/j.neuroimage.2008.12.037.

Krasuski, J.S., Alexander, G.E., Horwitz, B., Daly, E.M., Murphy, D.G.M., Rapoport, S.I., Schapiro, M.B., 1998. Volumes of medial temporal lobe structures in patients with Alzheimer's disease and mild cognitive impairment (and in healthy controls). Biol. Psychiatry 43, 60–68. https://doi.org/10.1016/S0006-3223(97)00013-9.

Kukolja, J., Thiel, C.M., Eggermann, T., Zerres, K., Fink, G.R., 2010. Medial temporal lobe dysfunction during encoding and retrieval of episodic memory in non-demented APOE ε4 carriers. Neuroscience 168, 487–497. https://doi.org/10.1016/j.neuroscience.2010.03.044.

Li, H., Karl, T., Garner, B., 2015. Understanding the function of ABCA7 in Alzheimer's disease. Biochem. Soc. Trans. 43, 920–923. https://doi.org/10.1042/BST20150105.

Liu, C.-C., Kanekiyo, T., Xu, H., Bu, G., 2013. Apolipoprotein E and Alzheimer disease: risk, mechanisms and therapy. Nat. Rev. Neurol. 9, 106–118. https://doi.org/10.1038/nrneurol.2012.263.

Mayeda, E.R., Glymour, M.M., Quesenberry, C.P., Whitmer, R.A., 2016. Inequalities in dementia incidence between six racial and ethnic groups over 14 years. Alzheimers Dement. J. Alzheimers Assoc. 12, 216–224. https://doi.org/10.1016/j.jalz.2015.12.007.

Mayeux, R., 2006. Genetic epidemiology of Alzheimer disease. Alzheimer Dis. Assoc. Disord. 20, S58–62. https://doi.org/10.1097/00002093-200607001-00008.

McLaren, D.G., Sperling, R.A., Atria, A., 2014. Flexible modulation of network connectivity related to cognition in Alzheimer's disease. NeuroImage 100, 544–557. https://doi.org/10.1016/j.neuroimage.2014.05.032.

Miao, J., Ma, H., Yang, Y., Liao, Y., Lin, C., Zheng, J., Yu, M., Lan, J., 2023. Microglia in Alzheimer's disease: pathogenesis, mechanisms, and therapeutic potentials. Front. Aging Neurosci. 15, 1201982. https://doi.org/10.3389/fnagi.2023.1201982.

Mucha, P.J., Richardson, T., Macon, K., Porter, M.A., Onnela, J.-P., 2010b. Community structure in time-dependent, multiscale, and multiplex networks. Science 328, 876–878. https://doi.org/10.1126/science.1184819.

Mucha, P.J., Richardson, T., Macon, K., Porter, M.A., Onnela, J.-P., 2010a. Community structure in time-dependent, multiscale, and multiplex networks. Science 328, 876–878. https://doi.org/10.1126/science.1184819.

Murrell, J.R., Price, B., Lane, K.A., Baiyewu, O., Gureje, O., Ogunniyi, A., Unverzagt, F. W., Smith-Gamble, V., Gao, S., Hendrie, H.C., Hall, K.S., 2006. Association of Apolipoprotein E Genotype and Alzheimer Disease in African Americans. Arch. Neurol. 63, 431–434. https://doi.org/10.1001/archneur.63.3.431.

Nakamura, A., Cuesta, P., Kato, T., Arahata, Y., Iwata, K., Yamagishi, M., Kuratsubo, I., Kato, K., Bundo, M., Diers, K., Fernández, A., Maestú, F., Ito, K., 2017. Early functional network alterations in asymptomatic elders at risk for Alzheimer's disease. Sci. Rep. 7, 6517. https://doi.org/10.1038/s41598-017-06876-8.

Nasciben, L.B., Nuytemans, K., Vasquez, M.L., Rajabli, F., Young, J.I., Dykxhoorn, D.M., Wang, L., Scott, W.K., Davis, D.A., Vontell, R.T., Pericak-Vance, M.A., Griswold, A.J., Vance, J.M., 2025. African origin haplotype protective for AD in APOEe4 carriers: exploring potential mechanisms. Alzheimers Dement 20, e091487. https://doi.org/10.1002/alz.091487.

Pasquini, L., Scherr, M., Tahmasian, M., Myers, N., Ortner, M., Kurz, A., Förstl, H., Zimmer, C., Grimmer, T., Akhrif, A., Wohlschläger, A., Riedl, V., Sorg, C., 2016. Increased intrinsic activity of medial-temporal lobe subregions is associated with decreased cortical thickness of medial-parietal areas in patients with Alzheimer's disease dementia. J. Alzheimers Dis. JAD 51. https://doi.org/10.3233/JAD-150823.

Power, J.D., Mitra, A., Laumann, T.O., Snyder, A.Z., Schlaggar, B.L., Petersen, S.E., 2014. Methods to detect, characterize, and remove motion artifact in resting state fMRI. NeuroImage 84. https://doi.org/10.1016/j.neuroimage.2013.08.048.

Prieto, S., Valerio, K.E., Moody, J.N., Hayes, S.M., Hayes, J.P., Alzheimer's Disease Neuroimaging Initiative, 2020. Genetic risk for Alzheimer's disease moderates the association between medial temporal lobe volume and episodic memory performance among older adults. J. Alzheimers Dis. JAD 76, 591–600. https://doi.org/10.3233/JAD-191312.

Rajabli, F., Feliciano, B.E., Celis, K., Hamilton-Nelson, K.L., Whitehead, P.L., Adams, L. D., Bussies, P.L., Manrique, C.P., Rodriguez, A., Rodriguez, V., Starks, T., Byfield, G. E., Lopez, C.B.S., McCauley, J.L., Acosta, H., Chinea, A., Kunkle, B.W., Reitz, C., Farrer, L.A., Schellenberg, G.D., Vardarajan, B.N., Vance, J.M., Cuccaro, M.L., Martin, E.R., Haines, J.L., Byrd, G.S., Beecham, G.W., Pericak-Vance, M.A., 2018. Ancestral origin of ApoE ε4 Alzheimer disease risk in Puerto Rican and African American populations. PLOS Genet 14, e1007791. https://doi.org/10.1371/journal.pgen.1007791.

Reitz, C., Jun, G., Naj, A., Rajbhandary, R., Vardarajan, B.N., Wang, L.-S., Valladares, O., Lin, C.-F., Larson, E.B., Graff-Radford, N.R., Evans, D., De Jager, P.L., Crane, P.K., Buxbaum, J.D., Murrell, J.R., Raj, T., Ertekin-Taner, N., Logue, M., Baldwin, C.T., Green, R.C., Barnes, L.L., Cantwell, L.B., Fallin, M.D., Go, R.C.P., Griffith, P., Obisesan, T.O., Manly, J.J., Lunetta, K.L., Kamboh, M.I., Lopez, O.L., Bennett, D.A., Hendrie, H., Hall, K.S., Goate, A.M., Byrd, G.S., Kukull, W.A., Foroud, T.M., Haines, J.L., Farrer, L.A., Pericak-Vance, M.A., Schellenberg, G.D., Mayeux, R., Alzheimer Disease Genetics Consortium, 2013. Variants in the ATP-binding cassette transporter (ABCA7), apolipoprotein E ϵ4,and the risk of late-onset Alzheimer

disease in African Americans. JAMA 309, 1483–1492. https://doi.org/10.1001/jama.2013.2973.

Rosenthal, S.L., Kamboh, M.I., 2014. Late-onset Alzheimer's disease genes and the potentially implicated pathways. Curr. Genet. Med. Rep. 2, 85–101. https://doi.org/10.1007/s40142-014-0034-x.

Saeed, U., Mirza, S.S., MacIntosh, B.J., Herrmann, N., Keith, J., Ramirez, J., Nestor, S.M., Yu, Q., Knight, J., Swardfager, W., Potkin, S.G., Rogaeva, E., St George-Hyslop, P., Black, S.E., Masellis, M., 2018. *APOE-ε4* associates with hippocampal volume, learning, and memory across the spectrum of Alzheimer's disease and dementia with Lewy bodies. Alzheimers Dement. J. Alzheimers Assoc. 14, 1137–1147. https://doi.org/10.1016/j.jalz.2018.04.005.

Sheldon, S., Levine, B., 2018. The medial temporal lobe functional connectivity patterns associated with forming different mental representations. Hippocampus 28, 269–280. https://doi.org/10.1002/hipo.22829.

Sinha, N., Berg, C.N., Tustison, N.J., Shaw, A., Hill, D., Yassa, M.A., Gluck, M.A., 2018. APOE ε4 status in healthy older african americans is associated with deficits in pattern separation and hippocampal hyperactivation. Neurobiol. Aging 69, 221–229. https://doi.org/10.1016/j.neurobiolaging.2018.05.023.

Sinha, N., Reagh, Z.M., Tustison, N.J., Berg, C.N., Shaw, A., Myers, C.E., Hill, D., Yassa, M.A., Gluck, M.A., 2019. ABCA7 risk variant in healthy older African Americans is associated with a functionally isolated entorhinal cortex mediating deficient generalization of prior discrimination training. Hippocampus 29, 527–538. https://doi.org/10.1002/hipo.23042.

Soldan, A., Pettigrew, C., Lu, Y., Wang, M.-C., Selnes, O., Albert, M., Brown, T., Ratnanather, J.T., Younes, L., Miller, M.I., Team, T.B.R., 2015. Relationship of medial temporal lobe atrophy, APOE genotype, and cognitive reserve in preclinical Alzheimer's disease. Hum. Brain Mapp. 36, 2826–2841. https://doi.org/10.1002/hbm.22810.

Sperling, R.A., Dickerson, B.C., Pihlajamaki, M., Vannini, P., LaViolette, P.S., Vitolo, O. V., Hedden, T., Becker, J.A., Rentz, D.M., Selkoe, D.J., Johnson, K.A., 2010. Functional alterations in memory networks in early Alzheimer's disease. NeuroMolecular Med 12, 27–43. https://doi.org/10.1007/s12017-009-8109-7.

Stepler, K.E., Gillyard, T.R., Reed, C.B., Avery, T.M., Davis, J.S., Robinson, R.A.S., 2022. ABCA7, a genetic risk factor associated with Alzheimer's disease risk in African Americans. J. Alzheimers Dis. JAD 86, 5–19. https://doi.org/10.3233/JAD-215306.

Sun, F.T., Miller, L.M., D'Esposito, M., 2004. Measuring interregional functional connectivity using coherence and partial coherence analyses of fMRI data. NeuroImage 21, 647–658. https://doi.org/10.1016/j.neuroimage.2003.09.056.

Telesford, Q.K., Lynall, M.-E., Vettel, J., Miller, M.B., Grafton, S.T., Bassett, D.S., 2016. Detection of functional brain network reconfiguration during task-driven cognitive states. NeuroImage 142, 198–210. https://doi.org/10.1016/j.neuroimage.2016.05.078.

Wolk, D.A., Das, S.R., Mueller, S.G., Weiner, M.W., Yushkevich, P.A., 2017. Medial temporal lobe subregional morphometry using high resolution MRI in Alzheimer's disease. Neurobiol. Aging 49, 204–213. https://doi.org/10.1016/j.neurobiolaging.2016.09.011.

Xie, L., Wisse, L.E.M., Das, S.R., Wang, H., Wolk, D.A., Manjón, J.V., Yushkevich, P.A., 2016. Accounting for the confound of meninges in segmenting entorhinal and perirhinal cortices in T1-weighted MRI. Med. Image Comput. Comput. Assist. Inter. MICCAI Int. Conf. Med. Image Comput. Comput. Assist. Inter. 9901, 564–571. https://doi.org/10.1007/978-3-319-46723-8_65.